Inclusive quarkonium production in pp - Experimental results

D. Hagan
With contributions from F. Damas and V. Zhovkovska.

QaT 2023
08/01/23

Introduction

- Cover the most up to date inclusive quarkonium cross-section results from pp at ATLAS, CMS, LHCb, and ALICE.
- Following on from QwG2022 and a similar review was presented at QCD@LHC by Valeriia Zhovkovska.
- Today I'll cover;
  - Detectors at pp experiments.
  - The structure of cross section analyses.
  - Estimating acceptance effects.
  - J/ψ, J/ψ polarisation
  - $\psi(2S)$.
  - Υ.
  - $\eta_c(1S, 2S)$.
  - χ_c, χ_c polarisation.

Detectors

- ATLAS
  - General purpose, $\sim 4\pi$sr, though suited to mid-rapidity studies.
  - Integrated luminosities of $139 fb^{-1}$ in Run 2, $37.8 fb^{-1}$ in 2022 Run 3.
  - Quarkonium studies here conducted with reconstruction of muon pairs.
  - Muon identifications are limited to 1 per RoI of $\Delta\phi \times \Delta\eta \approx 0.1$, effects on Υ trigger efficiency must be corrected for.

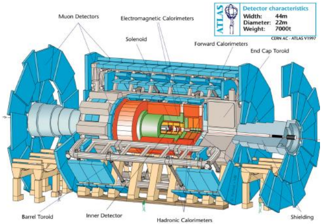

- CMS
  - General purpose, $\sim 4\pi$sr. 3.8T Similar mid-rapidity suitability as ATLAS
  - Quarkonium studies here conducted with reconstruction of muon pairs.
  - Forward calorimeters extend coverage out to $y < 5$.

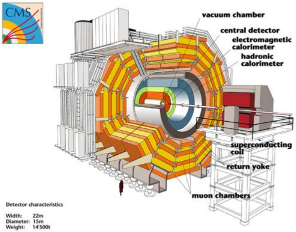

Detectors

- LHCb
  - Departure from the previous detectors, single arm construction.
  - Forward region studies, $2 < y < 5$, 4Tm Dipole Magnet.
  - Designed for studies of particles containing c and b quarks, very well suited to our explorations.
  - Reconstruction of quarkonium using hadronic channels extremely useful.
- ALICE
  - Designed for heavy-ion studies though some pp results are available.
  - These are typically used for baselining.
  - Design is suited to both forward and midrapidity studies.
  - More limited statistics associated with pp collisions

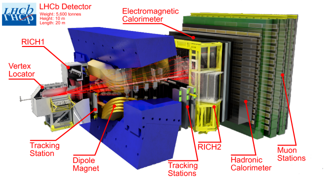

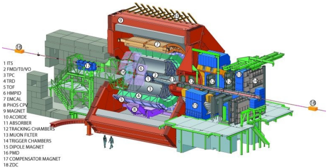

Quarkonium cross section measurements

- Beyond event selection and compensation for bin migrations, detector resolutions, trigger efficiencies, etc, measuring quarkonium cross sections in pp production is broadly the same across ATLAS, ALICE, CMS, and LHCb.
- Example from a $\sqrt{s} = 7, 8$TeV analysis at ATLAS - 1512.03657
- Firstly events with valid candidates are identified by selection cuts, the details of this vary depending on the kinematic region, signature, experimental setup, etc.
- After identifying candidates, their mass spectrum is reconstructed.
- When attempting to measure charmonium cross sections some measure of the charmonium decay vertex is required to help separate yields from prompt production and non-prompt contributions from b-decays.
- This measure can be pseudo-proper lifetime, decay length, and so on.
- One or both of these measures is used in a χ^2 or more typically a maximum likelihood fit, to extract the yield of quarkonium.

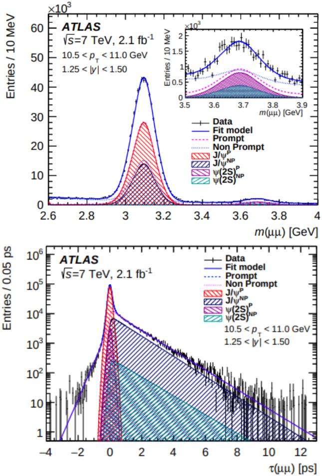

Quarkonium cross section measurements

- If we extract that yield differentially by performing the fits in bins of transverse momentum p_T and rapidity y, we can produce a double differential cross section.

$$\frac{d^2\sigma^{P,NP}}{dp_T dy} \times \mathcal{B}(\mathcal{Q}) = \frac{C}{A(\mathcal{Q})} \cdot \frac{N^{P,NP}_{\mathcal{Q}}}{\Delta p_T \Delta y \int \mathcal{L}dt}$$

- $\mathcal{B}$ is the branching fraction of quarkonia $\mathcal{Q}$ to the relevant final state, and $N^{P,NP}_{J/\psi}$ is the yield of the prompt and non-prompt fractions.
- $\frac{C}{A}$ is the ratio of a generic correction factor for various effects, to the acceptance for $\mathcal{Q}$
- ΔP_T and Δy are the widths of the transverse momentum and rapidity bins respectively, and $\int \mathcal{L}dt$ is the integrated luminosity.
- The results of this can be compared directly with theoretical predictions.

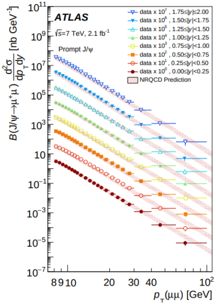

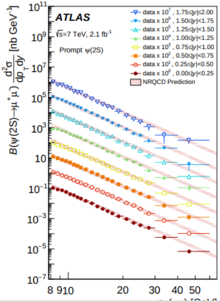

Maximum Likelihood fit

- Often, with the mass peaks of quarkonia being quite tightly grouped, even overlapping, it makes sense to measure a selection of them together.
- This involves careful construction of the p.d.fs used in the extraction of the yields in order to get a good match to the lineshape.
- Continuing with the ATLAS paper from before, when extracting J/ψ and $\psi(2S)$ in their prompt and non-prompt forms, along with identifying the backgrounds, use a complicated p.d.f.

$$PDF(m,\tau) = \sum_{i=1}^{7} \kappa_i f_i(m) \cdot h_i(\tau) \otimes R(\tau)$$

- Normalised such that $\Sigma\kappa_i = 1$. Each E_i has a differing decay constant. $f_i(m)$ is function for the mass and $h_i(\tau)$ for pseudoproper lifetime.
- Seven terms account for the four signal yields and three backgrounds. $R(\tau)$ represents a resolution function, and ω is the fractional share between the Bernstien Polynomials and Gaussian.

i	Type	Source	$f_i(m)$	$h_i(\tau)$
1	J/ψ	P	$\omega B_1(m) + (1-\omega)G_1(m)$	$\delta(\tau)$
2	J/ψ	NP	$\omega B_1(m) + (1-\omega)G_1(m)$	$E_1(\tau)$
3	$\psi(2S)$	P	$\omega B_2(m) + (1-\omega)G_2(m)$	$\delta(\tau)$
4	$\psi(2S)$	NP	$\omega B_2(m) + (1-\omega)G_2(m)$	$E_2(\tau)$
5	Bkg	P	F	$\delta(\tau)$
6	Bkg	NP	$C_1(m)$	$E_3(\tau)$
7	Bkg	NP	$E_4(m)$	$E_5(\|\tau\|)$

Notation	Function
G	Gaussian
CB	Crystal Ball
E	Exponential
B	Bernstein polynomials

Acceptance and polarisation

- Acceptance is the probability in cases where, say $J/\psi \to \mu^+\mu^-$, both muons pass the fiducial selection.
- With 2 muons, we have a dependence on 5 parameters, p_T, $|y|$, azimuthal angle ϕ of J/ψ, and two angles describing the $\mu\mu$ decay θ^*, and ϕ^*.
- θ^* is the polar angle between μ^+ in the J/ψ decay frame and the J/ψ in the lab frame. ϕ^* is the angle between the $\mu\mu$ production and decay planes in the lab frame.
- The following analytical result describes the decay distribution in the quarkonium rest frame for the $\mu\mu$ case.

$$\frac{d^2N}{d\cos\theta^*\phi^*} \propto 1 + \lambda_\theta \cos^2\theta^* + \lambda_\phi \sin^2\theta^* \cos 2\phi^* + \lambda_{\theta\phi} \sin 2\theta^* \cos\phi^*$$

- These λ_i parameters describe the spin-alignment state of the J/ψ, Υ, etc, in this decay mode.
- Whats important to experimentalists here is that there can be a strong dependence of the acceptance on the spin alignment state.
- To start accounting for this, identify the extreme polarisation cases.

	Angular coefficients		
	λ_θ	λ_ϕ	$\lambda_{\theta\phi}$
Isotropic *(central value)*	0	0	0
Longitudinal	−1	0	0
Transverse positive	+1	+1	0
Transverse zero	+1	0	0
Transverse negative	+1	−1	0
Off-(λ_θ–λ_ϕ)-plane positive	0	0	+0.5
Off-(λ_θ–λ_ϕ)-plane negative	0	0	−0.5

Acceptance and polarisation

- With the description of the decay distribution and the cases for each of the polarisations, we can start to generate acceptance maps.
- These acceptance maps are binned in P_T and $|y|$, and are created for each spin-alignment scenario.
- For each polarisation case, sample uniformly over θ^* and ϕ^* using a large number of events from generator-level simulations, weighted by the decay distribution, and record how many pass or fail the fiducial selection cuts.
- Shown right is the computed J/ψ acceptance for the 7, 8TeV ATLAS paper.
- The inverse value of the acceptance from each $p_T - |y|$ bin is then applied in the calculation of the double-differential cross section.
- Note that these corrections are typically made in a more averaged form to the cross section, in preference to supplying weight to the events being fit by the pdf. This is done to reduce any instability in the fit that might be introduced.

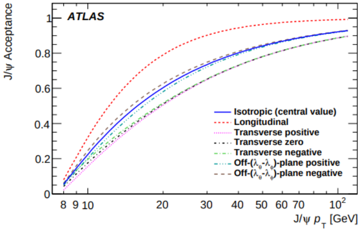

J/ψ polarisation - 1805.04374

- A forward rapidity study, with 1.23pb^{-1}, at ALICE, low P_T
- Measurement of λ_θ, λ_ϕ, and $\lambda_{\theta\phi}$ conducted as functions of P_T, in both helicity and collins-soper frame.
- Results align well with J/ψ being unpolarized across the P_T range. Reinforced with the P_T-integrated values.
- Tensions here with both NRQCD and CSM.

Parameter	HX frame	CS frame
$\langle\lambda_\theta\rangle$	-0.006 ± 0.115	0.012 ± 0.116
$\langle\lambda_\varphi\rangle$	-0.024 ± 0.058	-0.036 ± 0.053
$\langle\lambda_{\theta\varphi}\rangle$	-0.029 ± 0.047	-0.006 ± 0.047

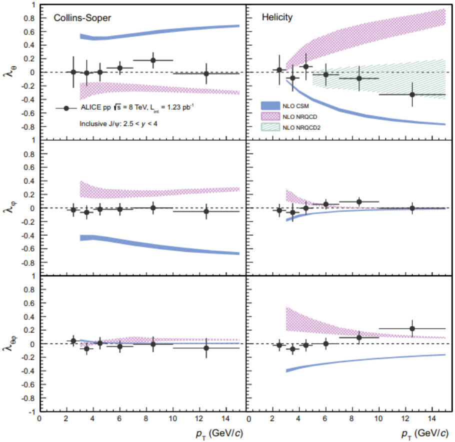

J/ψ at ATLAS - ATLAS-CONF-2019-047

- $\sqrt{s} = 13$TeV analysis, double-differential cross section produced from 139fb^{-1}, simultaneous analysis with $\psi(2S)$, discussed later.
- Previous $\sqrt{s} = 7, 8$TeV study, 1512.03657, utilised 4GeV cut triggers on muons, reached 100GeV until limited by trigger performance.
- Select J/ψ candidates using $\mu^+\mu^-$ with $P_{T,\mu_1} > 52.5$GeV and $P_{T,\mu_2} > 4$GeV.
- Emphasis here is on high-P_T, $60 - 360$GeV range, by using the higher P_T single muon trigger. $|y| < 2$,
- Vertex measure utilises pseudo-proper decay time $\tau = \frac{m \cdot L_{xy}}{P_T \cdot c}$.
- Events in the fit are weighted by the product of three weights, reconstruction, trigger efficiency, and decay-length correction.
- FONLL Model with default parameters matches data well, though cross sections in data are lower at the higher p_T end of the range.

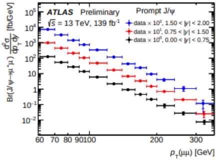

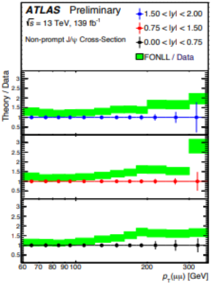

J/ψ at CMS - 1710.11002

- Narrower rapidity analysis than the previous ATLAS study with J/ψ candidate rapidity limited to $|y| < 1.2$.
- Non-prompt separation performed with the decay length $l = L_{xy} \cdot \frac{m_{J/\psi}}{p_T}$
- Mid P_T range search vs ATLAS paper, $\mu^+\mu^-$, with $P_{T,\mu} > 4.0 GeV$, and $|\eta| < 1.4$.
- Cut on muon P_T increased to 4.5GeV in the lower pseudorapidity region $|\eta| < 0.3$.
- Reaching out to forward regions is limited by trigger bandwidth.
- Double-differential cross-section ranges between $20 - 120$GeV. Integrating out rapidity increases upper limit to 150GeV.

- Comparison to NLO NRQCD produces good agreement across the full analysis range.

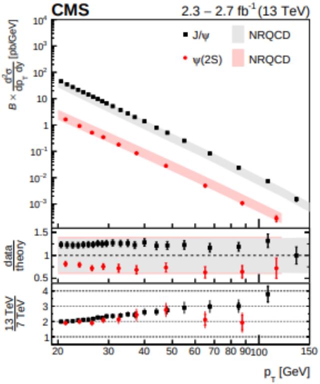

J/ψ at LHCb - 2109.00220

- $\sqrt{s} = 5$TeV analysis with 9.13fb^{-1} and $|P_T| < 20$GeV.
- As expected, forward rapidities $2.0 < y < 4.5$, two common vertex muon tracks $2.0 < \eta < 4.9$
- Requires muons of $P_{T,\mu} > 0.9$GeV and > 0.65GeV, total momentum $P > 3$GeV
- False track background reduced by neural network, dimuon invariant mass within 0.12GeV of J/ψ mass peak.
- Events restricted to a pseudo-proper time $|t_z| < 10$ps.
- Pseudo-proper time is analagous to the other lifetime measures, though it accounts for the foward regions accessed by LHCb.
- The absence of resolution in the transverse plane means the measure is constrained to be along the z-axis, the beamline.
- Tested FONLL and both NLO NRQCD and CGC + NRQCD models. Generally a good match to the data, though there is some small deviation in the low P_T region with the CGC+NRQCD modelling.
- Uncertainties associated with LDME calculation, and the factorisation and renormalisation scales are included in the NRQCD and CGC determinations.

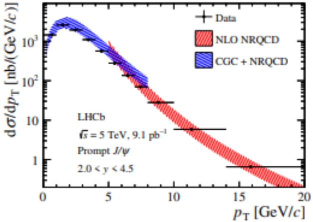

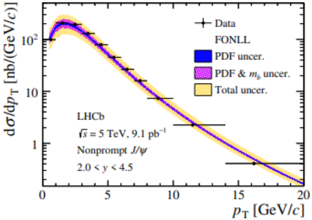

J/ψ at ALICE - 2108.02523

- $\sqrt{s} = 5.02, 13$TeV, with 19.4nb^{-1} and 32.2nb^{-1}, respectively. Statistics are limited here.
- Midrapidity study, $|y| < 0.9$, $P_{T,J\psi}$ extends down to 2Gev for the 5TeV data and as low as 1GeV for the 13TeV.
- J/ψ candidates formed using e^+e^- pairs now, and pseudo-proper decay length is used $x = \frac{c \cdot \vec{L} \times \vec{P_T} \cdot m_{J/\psi}}{|P_T|}$
- FONLL model agrees well with the data collected for non-prompt cross sections.
- ICEM, NRQCD+CGC, and NLO NRQCD, describe the data within uncertaites though note uncertainties due to luminosities are not included.

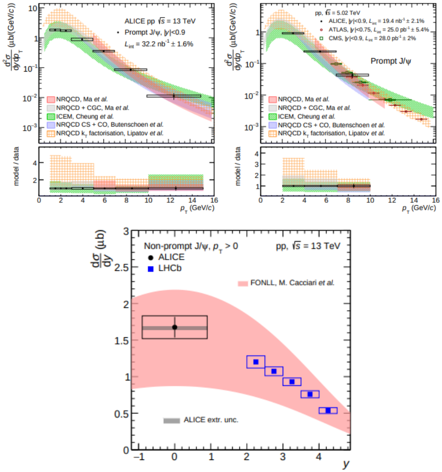

J/ψ at ALICE - 2109.15240, and summary

- Another cross section analysis for J/ψ is performed at ALICE, focussing on forward rapidities.
- At $\sqrt{s} = 5.02$TeV, with a dimuon approach, an integrated luminosity of 1229.9nb^{-1}.
- Tests of NRQCD, and ICEM all describe the extracted cross sections well.
- Note that the maximum-likelihood fit here focusses only on the mass.

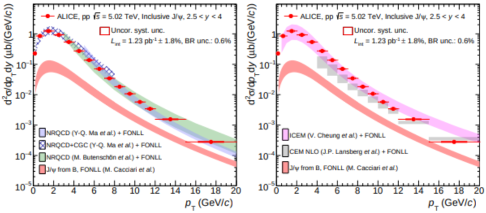

- To summarise, J/ψ quarkonium cross sections are well explored within pp experiments.
- NLO NRQCD, CGC+NRQCD, ICEM, and FONLL are all tested with J/ψ cross sections, all give a generally good agreement with the data.

$\psi(2S)$ at ATLAS - ATLAS-CONF-2019-047

- For $\psi(2S)$ ATLAS analysis procedure remains unchanged, extracted alongside the J/ψ in the same analysis.
- Use the same final state and a wide dimuon mass window, $2.6 < m_{\mu\mu} < 4.2$, such that both the J/ψ and $\psi(2S)$ mass peaks are included.
- $\psi(2S)$ is typically more difficult to extract, lower branching fraction, higher backgrounds, though it is a state with minimal pollution from feeddown.
- Non-prompt fractions and $J/\psi/\psi(2S)$ production ratios are also extracted. These are helpful in ratioing out acceptance effects in the cross sections.
- Spin-alignment parameters appear consistent with J/ψ, no polarisation.

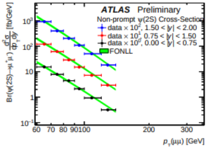

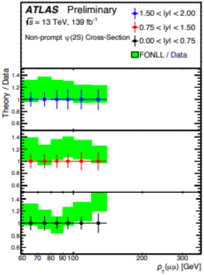

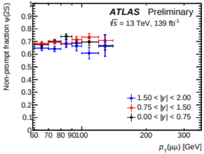

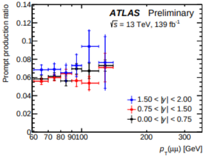

$\psi(2S)$ at CMS - 1710.11002

- As seen before;

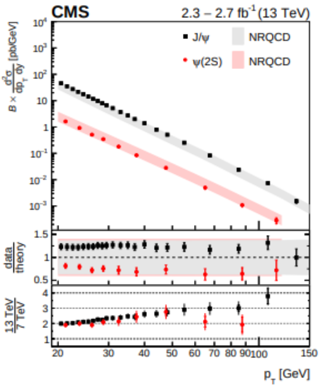

- Note the following picture of cross sections across differing rapidities have been scaled to be presented appropriately.

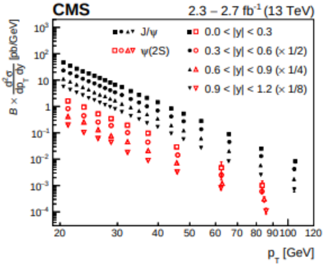

- NLO NRQCD shows good agreement in both J/ψ and $\psi(2S)$ data.

$\psi(2S)$ at LHCb - 1908.03099

- $\sqrt{s} = 7, 13\,TeV$. This LHCb analysis focusses only on $\psi(2S)$, with 275pb^{-1}
- Use a dimuon mass window to suit this; $3.566 < m_{\mu\mu} < 3.806$GeV.
- Same process as usual to produce the cross sections, reaching down to low P_T.
- Offline selection criteria between 7TeV and 13TeV are the same, allowing the maximum number of systematics to cancel in the cross section ratio. Very helpful for precision tests of theory.
- Also produced an estimate on the $b \to \psi(2S)$ branching fraction $\mathcal{B} = (3.08 \pm 0.02(stat) \pm 0.18(syst) \pm 0.27(\mathcal{B}))10^{-3}$
- Good performance of FONLL, though some tension at low P_T with NRQCD.

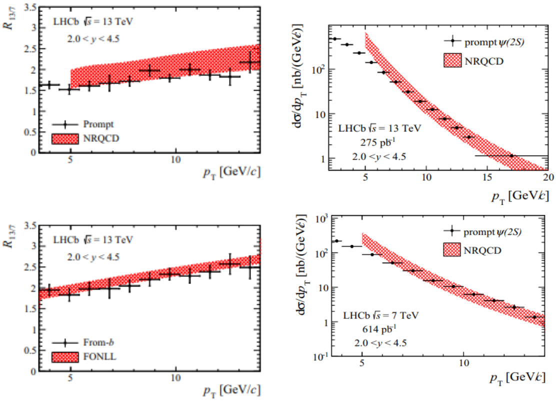

$\psi(2S)$ at ALICE - 2109.15240

- Return to the forward region ALICE analysis.
- Dimuon mass range includes both J/ψ and $\psi(2S)$ again, yield extraction shown here.

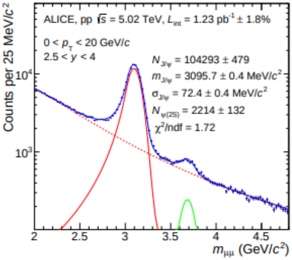

- Again, non-prompt and prompt are produced together, the non-prompt contributions here are predicted by previous studies into FONLL.

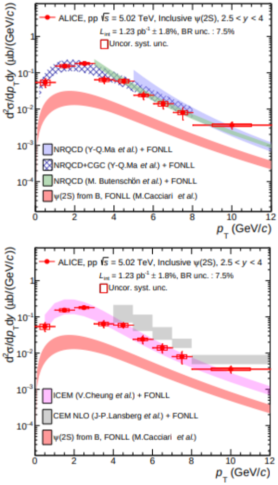

Υ Analyses and polarization - 1501.07750, 1709.01301

- A small modification must be made for the Υ case, measures of vertices used in separation of prompt and non-prompt no longer have meaning.
- We also have $\Upsilon(1S)$, $\Upsilon(2S)$, and $\Upsilon(3S)$. Mass peaks here are relatively close, sometimes overlapping.
- Comparisons of Υ cross sections with theory complement the lighter charmonium evaluations.
- Studies conducted at CMS and LHCb exclude large transverse or longitudinal Υ polarisation.

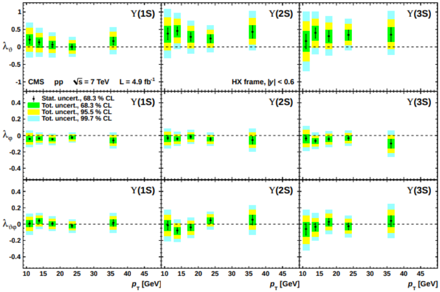

Υ at ATLAS - 1211.7255v2

- At ATLAS, no recent publication on Υ production of this form, though shown at QWG2022 was an exploration of the correlation of Υ production with UE, worth checking - ATLAS-CONF-2022-023.
- Most recent *pp* focussed paper at ATLAS, 2013, $\sqrt{s} = 7$TeV, $P_{T,\Upsilon} < 70$GeV.
- Measurement assumed $\lambda_\theta = \lambda_\phi = \lambda_{\theta\phi} = 0$
- Using 1.8fb^{-1} of data. Dimuon mass range shifted to $8 < m_{\mu\mu} < 11.5$GeV.
- This time use least squares fit on $\mu\mu$ spectrum that has been weighted by reconstruction efficiencies.
- Paper released a few months before the Υ polarisation results at CMS, fully longitudinal or transverse zero polarisation could have affected cross sections by $\pm 20\%$
- Also, some values of λ_ϕ would affect cross sections by upwards of 200%
- No tests of ICEM or NRQCD here, illustration of the importance of the polarisation effects.

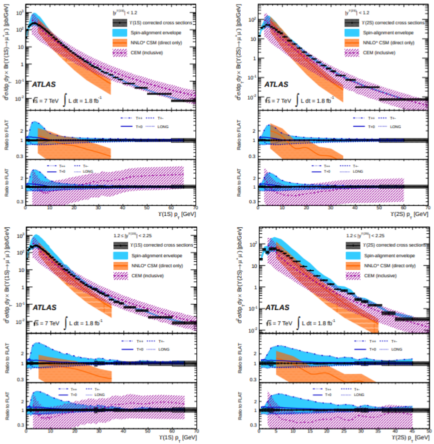

Υ at LHCb - 2212.12664

- Submitted to JHEP, not yet published!
- Examines $\sqrt(s) = 5$TeV with 9.13fb^{-1}.
- Returning to unbinned maximum likelihood fits, only on $m_{\mu\mu}$
- NRQCD evaluated with the $\Upsilon(1S)$ cross section. Theoretical predictions match well.

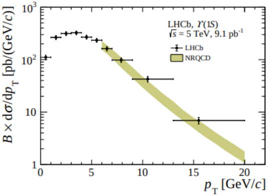

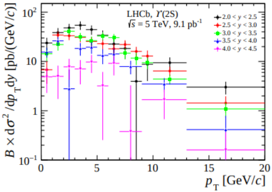

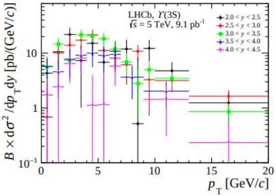

Υ at ALICE - 2109.15240

- The same forward rapidity ALICE paper as the previously shown. Likelihood fit is again limited to only $m_{\mu\mu}$
- First measurement at ALICE of $\Upsilon(1S)$ as a function of P_T and y.
- P_T integrated cross sections are also produced for $\Upsilon(1S)$, $\Upsilon(2S)$, and $\Upsilon(3S)$.
- This is due to statistical limitation on $\Upsilon(2S)$ and $\Upsilon(3S)$.
- A comprehensive exploration of ICEM is produced by this paper, good agreement in all cases.

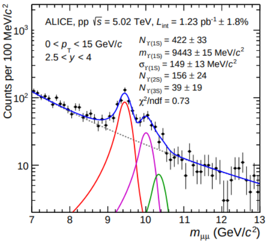

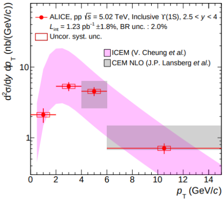

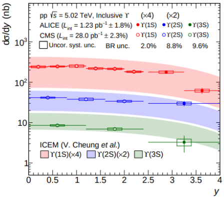

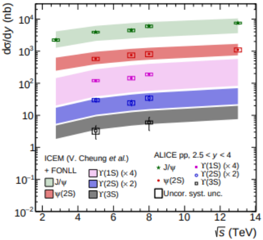

$\eta_c(1S)$ at LHCb - EPCJ 80 (2021) 191

- First $\eta_C(1S)$ prompt production cross section measurement at $\sqrt{s} = 13$TeV
- Forward rapidity measurement, $2.0 < y < 4.5$, at $6.5 < P_T < 14.0$GeV, with 2.0fb^{-1}.
- The previous analysis structure remains the same, though selection is altered as η_C is reconstructed from $\eta_c \to p\bar{p}$.
- Differential cross section for η_c is performed relatively to that of J/ψ.
- The possible background here changes from the $\mu\mu$ continuum to $J/\psi \to p\bar{p}\pi^0$ decays where π^0 is not reconstructed.
- Similar maximum-likelihood extraction with mass of $p\bar{p}$ pairs. Alternative analysis also featured extraction of prompt and non-prompt contributions.
- Described well by CSM, though difference in P_T dependence on cross section of η_c to J/ψ requires investigation, extend to higher P_T. CO contributions?

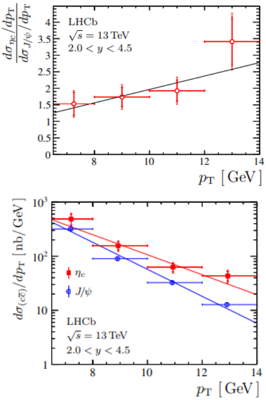

- Also extract $J/\psi - \eta_C$ mass difference to be $\Delta M_{J/\psi - \eta_C} = 113.0$MeV, provided most accurate mass determination.

$\eta_c(1S, 2S)$, $\chi_{c0,c1,c2}$ at LHCb using $\phi\phi$ - 1706.07013

- B-hadron focussed study, non-prompt production of all charmonium here. $\sqrt{s} = 7, 8$TeV with 3.0fb^{-1}.
- An additional step of reconstruction is required from use of $\phi\phi$ decay channel.
- This warrants the invariant mass of the ϕ pair be reconstructed from a 2D fit of each of the two K^+K^- distributions first.
- Yield is then extracted with a χ^2 fit to the rebuilt $M_{\phi\phi}$ distribution.
- Calculated yields used for comparison with theory do not account for feeddown from intermediate states.
- First measurement of $\eta_c(2S)$ in b decays, first measurement of branching fraction of χ_{c2}, and most accurate measurement of branching fraction of χ_{c1} in b decays.

$$\mathcal{B}(b \to \chi_{c0}X) = (3.02 \pm 0.47 \pm 0.23 \pm 0.94_{\mathcal{B}}) \times 10^{-3}$$
$$\mathcal{B}(b \to \chi_{c1}X) = (2.76 \pm 0.59 \pm 0.23 \pm 0.89_{\mathcal{B}}) \times 10^{-3}$$
$$\mathcal{B}(b \to \chi_{c2}X) = (1.15 \pm 0.20 \pm 0.07 \pm 0.36_{\mathcal{B}}) \times 10^{-3}$$

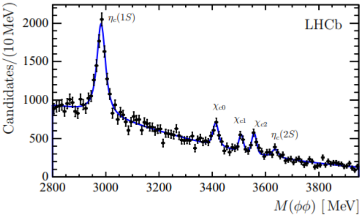

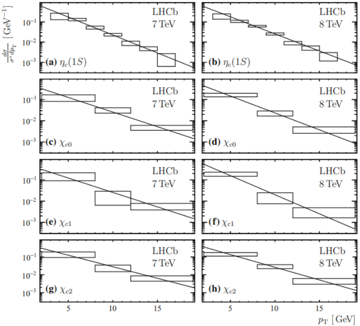

χ_c polarisation 1912.07706

- CMS measurement at $\sqrt{s} = 8$TeV with 19.1fb^{-1}.
- The first measurement of the polarizations of promptly produced χ_{c1} and χ_{c2}, and first measurement of significantly polarised quarkonia.
- Produced as ratios χ_{c2}/χ_{c1} in three seperate P_T bins from 8-30GeV.
- Matches NRQCD predictions, there is a notable difference between the parameters describing polar anisotropy $\lambda_\theta^{\chi_{c1}}$ and $\lambda_\theta^{\chi_{c2}}$
- Red region here are the physically allowed configurations, most of this is excluded.
- Easy to infer that one of the χ_c states is polarised, at minimum.
- $\chi_c \to \mu^+\mu^-$ not covered yet for cross sections or polarisations.

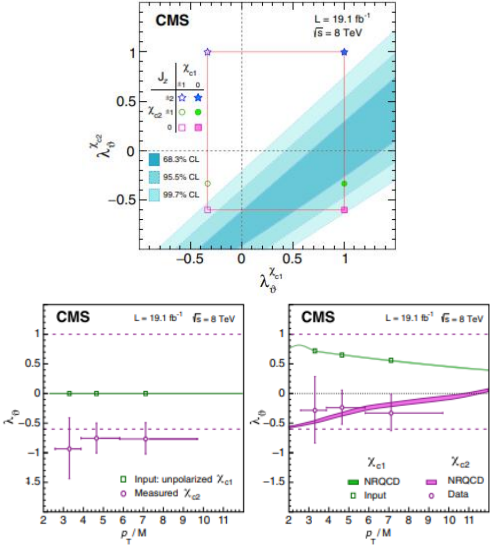

$\chi_{c1,2}$ at ATLAS - 1404.7035v2

- $\sqrt{s} = 7$TeV measurement of χ_{c1} and χ_{c2} with 4.5fb^{-1}
- Another variation on measurement, using $\chi_{cn} \to J/\psi + \gamma$. γ is reconstructed through e^+e^- and J/ψ through $\mu^+\mu^-$
- $J/\psi + \gamma$ events from sources outside of χ_c are rejected by requiring impact parameter of the photon w.r.t the J/ψ candidate vertex be less than 5mm.
- The two dimensional unbinned likelihood fit uses $m_{\mu^+\mu^-\gamma} - m_{\mu^+\mu^-}$ and pseudoproper lifetime.
- Differential cross-sections in both $P_{T,J/\psi}$ and P_{T,χ_c} are produced using the same process.
- Prompt and non-prompt production kinematics of χ_{c1} and χ_{c2} are different so the acceptance correction is adjusted per yield.
- Good agreement with of both χ_{c1} and χ_{c2} data to NLO NRQCD and FONLL predictions.

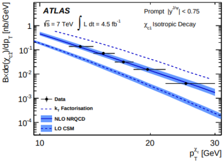

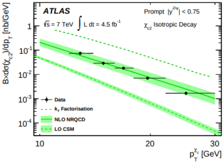

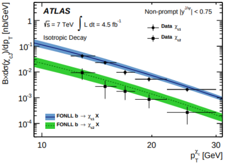

$\chi_{c1,2}$ at CMS - 1210.0875

- $\sqrt{s} = 7$TeV measurement of χ_{c1} and χ_{c2} with 4.6fb^{-1}
- $\chi_{c1,c2} \rightarrow J/\psi + \gamma$ again.
- Maximum likelihood fit nearly identical to ATLAS case, only applied to the mass measure, uses a slightly different configuration defining $Q = m_{\mu^+\mu^-\gamma} - m_{\mu^+\mu^-} + m_{J/\psi}$
- Analysis focusses solely on prompt production, selects only events with transverse decay length $L_{J/\psi} = L_{xy} \cdot \frac{m_{J/\psi}}{p_{T,J/\psi}} < 30\mu$m
- NRQCD here describes the data well.

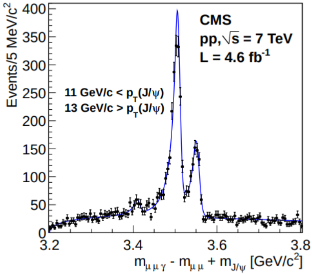

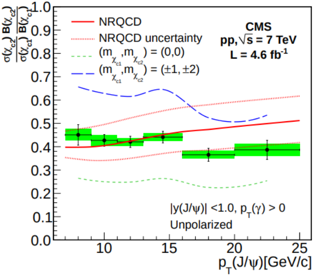

Conclusion

- To summarise, there is a well-established formula for extracting quarkonium cross section in pp experiments.
- This extends to the how we manage acceptances, backgrounds, and extracting yields.
- Broad spectrum of results across rapidities and kinematic regions are complementary to each other and provide valuable information when it comes to evaluating theoretical models of production.
- In most tests there is good agreement of theory and data, though some small tensions are present.
- There are more results on the way!

Conclusion

- To summarise, there is a well-established formula for extracting quarkonium cross section in pp experiments.
- This extends to the how we manage acceptances, backgrounds, and extracting yields.
- Broad spectrum of results across rapidities and kinematic regions are complementary to each other and provide valuable information when it comes to evaluating theoretical models of production.
- In most tests there is good agreement of theory and data, though some small tensions are present.
- There are more results on the way!

Thanks for listening!

Results Summary

Thanks for listening!

- J/ψ - 1805.04374, ATLAS-CONF-2019-047, 1710.11002, 2109.00220, 2109.00220, 2108.02523, 2109.15240.
    - Polarisation parameters consistent with 0.
    - Explored over all P_T ranges and rapidities.
    - NRQCD and ICEM produce good matches across all y and P_T ranges.
    - Some tension in FONLL at high P_T
- $\psi(2S)$ - 1805.04374, ATLAS-CONF-2019-047, 1908.03099, 2109.15240.
    - Very similar status to J/ψ
    - Polarisation parameters consistent with J/ψ
    - Good agreement with NRQCD in mid to high P_T's, at low P_T some adjustment is required.
    - FONLL and ICEM perform well.
- Υ - 1501.07750, 1709.01301, 1211.7255v2, 2212.12664, 2109.15240.
    - Large polarisations are excluded.
    - Recent studies are forward rapidity
    - Good behaviour of ICEM and NRQCD.
- η_c - EPCJ 80 (2021) 191, 1706.07013.
    - Forward rapidity studies.
    - Well described by CSM.
    - Need to extend measurement to higher p_T
- χ_c - 1706.07013, 1912.07706, 1404.7035v2, 1210.0875.
    - Studied at middle and forward rapidities.
    - $\chi_c \to \mu^+\mu^-$ not covered for cross sections.
    - Good agreement of NRQCD and FONLL here.

Let me know if I've missed anything!